Scilight

Thermal Science and Applications
https://www.sciltp.com/journals/tsa



Article

Return Temperature Prediction in District Heating Networks Using Primary Side Measurement Data

Julia Eicke [1], Lina Eicke-Kanani [2], Alessandro Maccarini [3], Frank Dammel [1,*] and Peter Stephan [1]

[1] Institute for Technical Thermodynamics, Department of Mechanical Engineering, Technical University of Darmstadt, Peter-Grünberg-Str. 10, 64287 Darmstadt, Germany
[2] Center for Cognitive Science, Department of Psychology, Technical University of Darmstadt, Alexanderstr. 10, 64289 Darmstadt, Germany
[3] Department of the Built Environment, Faculty of Engineering and Science, Aalborg University, A.C. Meyers Vænge 15, 2450 Copenhagen, Denmark
* Correspondence: dammel@ttd.tu-darmstadt.de

How To Cite: Eicke, J.; Eicke-Kanani, L.; Maccarini, A.; et al. Return Temperature Prediction in District Heating Networks Using Primary Side Measurement Data. *Thermal Science and Applications* **2026**, *1*(3), 315–330. https://doi.org/10.53941/tsa.2026.100019

Received: 8 July 2026
Revised: 2 September 2026
Accepted: 17 September 2026
Published: 30 September 2026

Abstract: District heating networks are essential for decarbonizing the heating sector, yet their efficient operation is often hindered by high return temperatures, which indicate reduced efficiency or substation faults. Modeling return temperature is therefore critical but challenging due to complex building-side dynamics, limited data availability, and the high effort required for detailed physical simulations. This study proposes a measurement-based surrogate modeling approach for predicting primary side return temperature at substations in district heating networks. Our method is based on a simplified thermodynamic formulation of return temperature as a function of supply temperature, heat flow, and a scaling coefficient. A polynomial regression model is used to estimate this coefficient from primary side measurement data that are typically available to network operators, without relying on secondary side or building-specific information. Model performance is evaluated using residual analysis as well as statistical and goodness-of-fit metrics. The results demonstrate that our simple approach produces unbiased and accurate predictions of return temperature indicating that patterns arising from the system's behavior are captured despite the model's simplicity. The proposed approach provides a transferable and data-efficient alternative for scalable district heating network analysis under realistic data availability constraints. Our findings complement other conceptual contributions, highlighting the relevance of relatively simple statistical models to generate testable hypotheses for high-effort physical simulations.

Keywords: district heating; surrogate modeling; return temperature prediction; polynomial regression; data-driven modeling

1. Introduction

District heating plays a major role in the decarbonization of the heating sector. District heating networks supply heat to buildings while promoting energy-efficiency through the integration of multiple heat sources. However, their full potential remains unexploited due to high network temperatures, inflexible operation strategies and a reliance on fossil fuels for heat generation [1]. Unlocking their potential requires a comprehensive understanding of the entire system and the interactions between its components. Models of district heating networks, for example commonly used physical simulation models, can be used to replicate real-world behavior and are therefore employed to investigate operation strategies, detect faults via measurement data or to improve the network's performance. However, running detailed physical simulations entails high modeling effort due to

Copyright: © 2026 by the authors. This is an open access article under the terms and conditions of the Creative Commons Attribution (CC BY) license (https://creativecommons.org/licenses/by/4.0/).
Publisher's Note: Scilight stays neutral with regard to jurisdictional claims in published maps and institutional affiliations.

extensive data requirements, the need for expert system knowledge, and the solution of complex physical equations, which is computationally expensive in terms of time and computing resources.

Regarding district heating networks, the modeling effort increases strongly with network size, which is proportional to the number of connected buildings. Although the interaction between buildings and the network via substations remains a key determinant of system behavior (affecting return temperatures, mass flows, and pressure requirements) explicitly modeling internal building processes and detailed substation characteristics introduces substantial complexity. For higher-level analyses of overall system performance, it is therefore both appropriate and often necessary to abstract from internal building processes and focus on the actual network. This abstraction of the network can be achieved by replacing detailed physical models with surrogate models that provide desired outputs based on selected inputs relying on simple equations, as opposed to explicitly replicating all sub-systems. Surrogate models allow investigations of system behavior, while simultaneously omitting detailed physical equations and internal dynamics that have limited influence on the network level behavior under investigation.

Studies on building design and building performance have emphasized the importance of surrogate models as an appropriate representation of physical processes. Westermann and Evins [2] as well as Østergård et al. [3] and Zouloumis et al. [4] concluded that surrogate models are consistently shown to be significantly faster than detailed physical simulation models while still allowing the incorporation of physical knowledge. Furthermore, Boussaid et al. [5] showed that even extended frameworks combining several surrogate models—simulating consumers, producers and pipes—drastically reduce simulation time compared to step-by-step physical simulations. Overall, in the studies cited above surrogate models are believed to be crucial for obtaining meaningful and, in particular, explainable results.

Surrogate models predominantly rely on descriptive statistical methods, such as linear regression, as well as machine-learning-based models, i.e., artificial neural networks (ANNs) and support vector machines. While machine learning models often achieve higher predictive accuracy than simpler prediction approaches, both Westermann and Evins [2] and Zhao and Magoulès [6] report that they are also associated with higher model complexity, reduced interpretability and require extensive model training. In contrast, conventional statistical methods provide reasonable accuracy with substantially lower implementation effort and increased explainability [6], explaining their continued popularity. Consequently, this approach was adopted in the present work due to its balance of accuracy, simplicity, and interpretability.

Additionally, surrogate models that avoid large data requirements are particularly desirable, as they enable transferable, data-efficient modeling of district heating systems across different networks and applications. As a result, usual data availability should be taken into account in the developing process to avoid constraints in the application for these models. In other words, a modelling approach ideally requires input variables which are commonly recorded in the field. Regarding district heating networks, constraints on data availability arise as secondary side data is typically not recorded, and detailed information on buildings or substations is frequently unavailable, as data collection is performed by network operators and therefore mainly focuses on data for billing and system monitoring purposes, such as primary side heat flow and supply and return temperatures. Consequently, modelling approaches based on secondary side operation or other building-specific information tend to have limited generalizability.

Given the discussed limitations of commonly available district heating network data, various studies successfully excluded building-specific and secondary side data and employed simple statistical models to predict heat demand using weather-related input variables instead.

Fang and Lahdelma [7] compared multiple linear regression and autoregressive models for citywide demand forecasting based solely on weather and heat consumption data. Comparable approaches were reported by Oltmanns [8] and Popescu et al. [9], who achieved satisfactory prediction accuracy using weather data and, in the latter case, simplified assumptions regarding indoor temperature.

While the aforementioned literature focuses predominantly on modeling heat demand, primary side return temperature in fact might be even more relevant for network operators since high return temperatures indicate reduced system efficiency or faulty substations, both of which are undesirable [10]. The importance of accurate return temperature representation is further supported by the work of Vandermeulen et al. [11], who conclude that return temperature is the key variable that must be properly modeled to represent substations.

Compared to heat demand, return temperature is considerably more complex to model, as it is influenced to a greater extent by heating system characteristics rather than by weather conditions. Consequently, measurement data is inherently noisier and subject to greater uncertainty. This variability is mediated by hidden dynamics inside the building such as control settings, or radiator sizing but also by unobserved factors with unclear context, which complicates the identification of suitable predictor variables.

As a result, various assumptions and modeling approaches have been proposed to represent return temperature in substation models, e.g., constant return temperatures [12], constant temperature differences

between supply and return temperature [13], estimations by neural networks [14] as well as linear relations with heat demand and primary supply temperature [15].

Vandermeulen et al. [11] propose that assuming a constant temperature difference at the primary side of the substation is not suitable for modeling substation behavior. In their study, they compared simulation models of substations with increasing levels of simplification, including one that required only heat demand and primary supply temperature as simulation input. The input data was created from a detailed simulation model, which served as benchmark model. While they effectively managed to map primary return temperature as a function of heat demand and primary supply temperature, secondary-side data was nevertheless required in the development of the model.

Notably, the studies [5,11–13,15] implemented return temperature as output variable, relying on synthetic data generated from physical simulation models as benchmark or source for input data, either generic or inspired by real-world systems. They therefore do not assess the suitability of the underlying return temperature assumptions in the context of real-world operating conditions. Overall, surrogate modeling studies that explicitly consider return temperature as an output variable remain scarce, particularly those incorporating measurement data from operational district heating networks.

Balancing the need for detailed representations with the desire for low-complexity and scalable models is crucial to keeping modeling effort and computation time manageable, especially when the research focus is on broader network-level phenomena rather than individual building dynamics. In this context, simple statistical or numerical models often outperform machine learning approaches due to their significantly lower implementation effort and higher interpretability. Simpler models thus offer advantages in deriving system-understanding, which is limited in higher level approaches, especially when employing ‘black box’ methods like ANNs.

The purpose of the current work is to provide a simplified model of a substation using conventional statistical approaches to reduce both model complexity and the amount of data required to predict primary side return temperature. To make our approach usable across different datasets, we aim to match common conditions under which data from district heating networks is generated, most often related to billing purposes. Therefore, all investigations were conducted based on primary side heat flow, supply and return temperature. The objective is to find a trade-off between model accuracy and practical applicability, ensuring robust return temperature predictions even under constraints of realistic data availability.

2. Methodology

The objective of the proposed methodology is to develop a measurement-data-based surrogate model for the primary side of substations in district heating networks. The motivation is to enable simplified modeling of overall systems while considering actual data availability; specifically limiting the necessary parameters to heat flow, supply and return temperature. This chapter presents the core principles of the modeling approach and the processing steps applied to the raw measurement data.

All of the work was implemented in Python (version 3.12.3). Numerical computations and data processing were performed using NumPy (version 2.4.2), Pandas (version 2.2.2) and Statsmodels (version 0.14.6), while model fitting and application as well as the statistical analyses were primarily conducted using functions from Scikit-Learn (version 1.8.0) and SciPy (version 1.17.0).

First, the origin of the data is set out in Section 2.1 followed by the description of the procedures for preprocessing and outlier treatment (Section 2.2). In Section 2.3 the data is further processed to obtain aggregated annual data per heating meter that represents average characteristics per heating meter. In Section 2.4 the modeling approach is introduced, including the model definition and its application procedure, as well as the approach used for the analysis of model performance.

2.1. District Heating Network and Dataset Description

The data used in this study was collected at the district heating network of Technical University of Darmstadt (Darmstadt, Germany). In this network the heat supply is covered by a generation plant consisting of combined heat and power plants paired with gas boilers, which distributes heat via five separate supply lines into five subgrids. Additionally, heat is supplied from the municipal waste incineration plant via a heat exchanger to one of the subgrids. Residual heat from the cooling of a high-performance computer is also fed into the network to pre-heat the returning mass flow before entering the generation plant. This additional heat supply, however, is negligible compared to the other sources and is not considered in this work.

The examined dataset included heat flow, return and supply temperature data from 135 heating meters installed at the primary side of the buildings’ substations. The period covered by the evaluated data ranged from

2018 to 2024. Additionally, measurement data was available at the supply lines from the generation plant as well as at the heat exchanger providing heat from the waste incineration plant.

The original recording resolution of 1 sample per 15 min was downsampled to hourly averages to reduce the amount of data and to match the more common resolution of 1 sample per hour. (Note that in the application of the method not all of the available data was used, see Section 2.4.2)

2.2. Data Cleaning

Measurement data of in-operation systems (especially long-term systems like district heating networks) are prone to outliers induced by unmonitored effects, e.g., environmental changes or (unknown) faults in system components. Additionally, the data are often noisy due to the dynamic nature of district heating systems, where fluctuating heat demand, control actions at substations and heating plants, as well as transient hydraulic and thermal effects cause short-term variations in the measurements. This noise makes it particularly difficult to discern between physically plausible effects and erroneous artifacts. Therefore, prior to conducting any analysis, the data of each heating meter are processed individually to remove outliers and fill missing values.

The preprocessing pipeline entailed two steps: first, we applied four criteria (see below) to remove physically implausible data and second, we applied a decomposition analysis to clean remaining data points outside the usual range of the bulk of data. Before and after each removal step, gaps in the time series of up to 5 h were linearly interpolated individually for each variable, such that the overall procedure follows the order illustrated in Figure 1. The details of the preprocessing are explained in the following.

Criteria for identifying physically implausible data points as outliers were:

(1) Samples that contained heat flow values below zero
(2) Samples where the supply temperature exceeded the overall highest temperature supplied by the generation plant within the observed timespan
(3) Samples where the return temperature exceeded the overall highest temperature supplied by the generation plant within the observed timespan
(4) Samples where the heat flow exceeded the highest installed building load

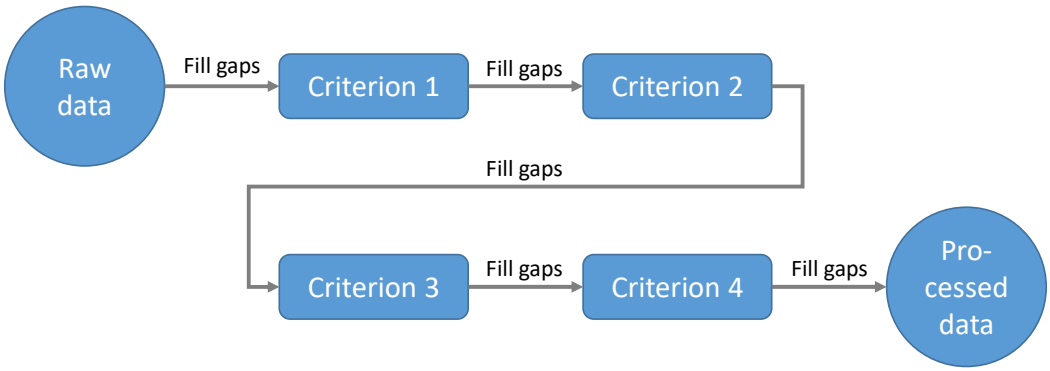


Figure 1. Schematic representation of data processing.

After cleaning the data according to criteria 1 to 4, visual inspection indicated that most observations lay within physically plausible ranges; however, manual examination revealed that some individual data points were outside the usual range of the bulk of data points. To further filter those values from the dataset we applied decomposition of time series in an additional preprocessing step.

The decomposition of time series is a statistical technique used to separate time series into distinct components: a trend component, a seasonal component and a residual component. The trend component reflects the long-term evolution of the data over time (e.g., year-to-year changes), while the seasonal component captures systematic, recurring patterns such as annual cycles. The residual component comprises irregular fluctuations that cannot be attributed to either the trend or seasonal effects.

Several approaches exist to combine these components. In this work, an additive decomposition model was employed, which assumes that the observed time series value $Y(t)$ can be expressed as the sum of an overall trend $T(t)$, seasonal variations $S(t)$ and irregularities covered in a residual term $e(t)$:

$$Y(t) = T(t) + S(t) + e(t). \quad (1)$$

Applying the decomposition model requires specifying a period that reflects the dominant seasonality of the data. For heating data, a yearly seasonal pattern was assumed, and the period was therefore set to 8760 h. The decomposition model was fitted separately to the time series of each variable for each heating meter.

As deviations not explained by trend or seasonality are captured in the residual component, $e(t)$ can be used to identify potential outliers. However, since such irregularities, may also arise from normal system operation, not all deviations in the residual component necessarily represent true outliers and must therefore be treated with caution. To be certain that we exclude real outliers, we removed data points where the z-scored residual components were outside of the interval of $[-3, 3]$ (i.e., outside of three standard deviations, based on the expected range of an approximately standard normal distribution). Resulting gaps in the time series of up to five hours were then imputed using linear interpolation.

A final visual/manual inspection of the processed data indicated that the applied outlier removal and interpolation steps result in a consistent and physically plausible time series.

2.3. Creating a Reference Year Dataset

The data cleaning revealed that while the heating meter measurements exhibit a recurring seasonal structure year-over-year, they display variability in magnitude and timing which result in individual annual characteristics, the cause of which can hardly be traced. Furthermore, several heating meter records still contained large, random data gaps across different years.

To construct a robust, generalizable model, the dataset was condensed by averaging hourly values across all available years. This approach suppresses year-specific anomalies to isolate typical operational profiles while simultaneously mitigating missing data issues. Consequently, it yields a standardized time-series dataset over an aligned time frame. Importantly, this strategy maximizes the usable number of heating meters, as many individual records lacked complete data across all monitored years.

To this end, the data of each variable of each heating meter were aggregated independently to represent average annual behavior of the observed timespan. Specifically, each measurement was detached from its original timestamp and reassigned to the corresponding hour of the year at which it was recorded (i.e., 1–8760). For example, a measurement recorded at 9:00 a.m. on 1 January was mapped to the 9th hour of the year, regardless of the calendar year in which it was collected. For each hour of this generic year, the mean was computed from the individual measurements of the heating meter. The resulting time series represents a typical annual pattern for the specific heating meter and is hereafter referred to as ‘reference data’ and the generic year as ‘reference year’. An example for the resulting reference data of heat flow, supply and return temperature is given in Figure 2. The grey dots indicate the measurement data, while the blue dots indicate the reference data, i.e., the average value for the corresponding hour of a year. It can be observed that general patterns in the data are captured. The obtained reference data is therefore used in the application of the following approach.

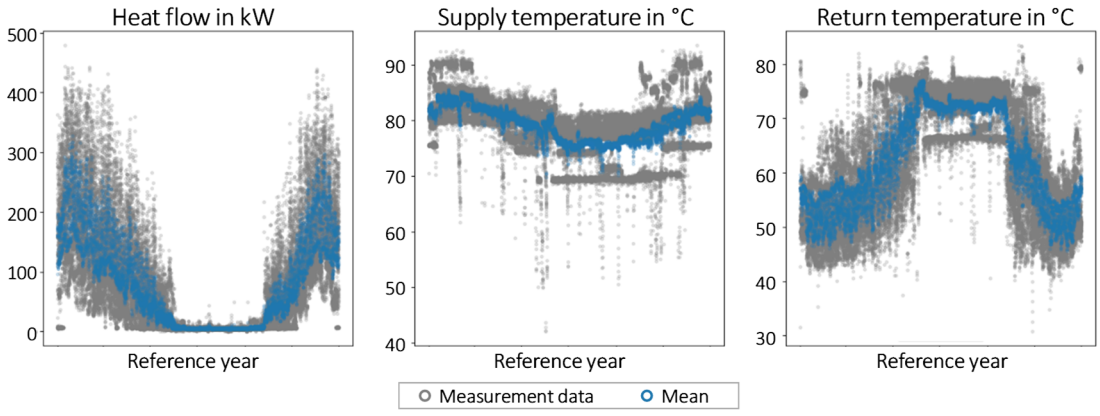


Figure 2. Example of processed measurement data (grey) and aggregated reference data (blue).

2.4. Modeling Approach

The basic modeling approach to predict return temperature was conceptualized based on the relationship of primary return temperature with primary side heat flow and supply temperature. In real-world operation these variables are most commonly coupled through heat exchangers located in the building’s substations, where heat from the primary side of the district heating network is transferred to the secondary side. This connection can be implemented through various configurations involving one or more heat exchangers, e.g., for separate space

heating and hot water preparation. The modeling approach in this work seeks to replace detailed substation configurations, aiming to generalize rather than specialize in actual layouts. For this reason, a single-heat-exchanger configuration serves as the baseline to capture the fundamental physical coupling. Figure 3 visualizes this simplified coupling, illustrating the heat flow that is transferred from the primary (red/blue) to the secondary side (orange/light blue).

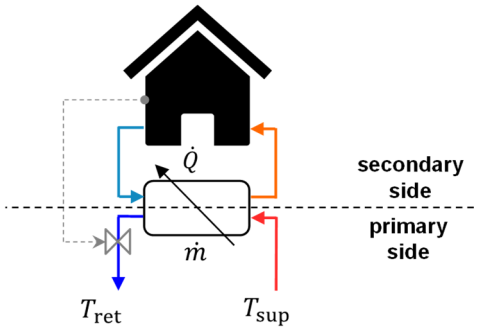


Figure 3. Schematic of a single-heat-exchanger substation connecting primary and secondary side via a heat exchanger.

In this process, the thermal energy from the generation plant is carried by the mass flow $\dot{m}$ through the primary side of the heat exchanger. As the heat flow $\dot{Q}$ is transferred to the, the mass flow temperature decreases from the supply temperature T_{sup} (red) at the inlet to the return temperature T_{ret} (blue) at the outlet of the heat exchanger. The mass flow rate is controlled by adjusting a valve (grey) on the primary side, so that the temperature requirements on the secondary side are met. In the following the role of each of the variables in substation operation is discussed and the considerations leading to the model definition are rolled out.

2.4.1. Definition of the Model and Assumptions About Network Influence

Like many other district heating networks, our university's network is mainly supplied by a centralized generation plant that adjusts the supply temperature using a heating curve based on the outside temperature. From a substation point of view this means that the supply temperature in the system is a globally set variable that is not affected by any of the substations' characteristics.

Since previous studies successfully showed that heat demand for individual buildings can be predicted solely based on weather parameters (see Section 1, refs. [7–9]), we assume that heat flow, like the supply temperature, can be considered equally unaffected by substation characteristics.

In contrast, the substations' properties do impact the primary side mass flow based on secondary side parameters. As a result, the secondary side adjustment of primary side mass flow represents the operation of the overall building's heating system and directly affects the resulting return temperature on the primary side. Consequently, the return temperature captures the combined effect of heat demand and substation efficiency, making it the key variable of the system.

The relationship between heat and mass flow and supply and return temperature on the primary side of a building, can be described using the general heat flow equation:

$$\dot{Q} = c_{\mathrm{w}}\dot{m}(T_{\mathrm{sup}} - T_{\mathrm{ret}}), \tag{2}$$

where c_W denotes the specific heat capacity of water.

By rearranging Equation (2) to T_{ret} one can observe that the return temperature can be expressed as the difference between the supply temperature T_{sup} and the heat flow $\dot{Q}$ multiplied by a scaling coefficient θ:

$$T_{\mathrm{ret}} = T_{\mathrm{sup}} - \dot{Q} \cdot \theta, \tag{3}$$

where

$$\theta = \frac{1}{c_{\mathrm{w}}\dot{m}}. \tag{4}$$

The parameter θ can therefore be interpreted as a dynamic system-specific coefficient that scales $\dot{Q}$ to account for systematic variations in mass flow, induced by, e.g., substation operation, hydraulic resistance and heat exchanger efficiency, so that values for T_{sup} can be mapped onto values for T_{ret}. Note that θ is a purely descriptive parameter to link heat flow, supply and return temperature and that we make no mechanistic assumptions which exact parts of the network influence it.

Consequently, predicting θ enables the computation of the respective T_{ret} based solely on primary side information, namely $\dot{Q}$ and T_{sup}. At this point a conceptual difficulty becomes apparent. While θ can be expressed as:

$$\theta = \frac{T_{\mathrm{sup}} - T_{\mathrm{ret}}}{\dot{Q}} \Longrightarrow f\left(\frac{T_{\mathrm{sup}}}{\dot{Q}}, \frac{T_{\mathrm{ret}}}{\dot{Q}}\right), \tag{5}$$

T_{ret} itself is the variable of interest. This creates a circular dependency.

As a result a regression model is defined, so that $\theta \approx \tilde{\theta} = f\left(\frac{T_{\mathrm{sup}}}{\dot{Q}}\right)$, where the information contained in T_{ret} is implicitly captured by the regression coefficients β_i. The model is formulated as:

$$\tilde{\theta} = \beta_0 + \beta_1 \frac{T_{\mathrm{sup}}}{\dot{Q}} + \beta_2 \left(\frac{T_{\mathrm{sup}}}{\dot{Q}}\right)^2. \tag{6}$$

The second order approach provides flexibility to approximate a wider range of functional relationships without introducing excessive model complexity. This allows for the consideration of non-linear characteristics, such as those typically found in district heating substations.

Eventually, the return temperature can be calculated using $\tilde{\theta}$, so that:

$$T_{\mathrm{ret}} \approx \tilde{T}_{\mathrm{ret}} = T_{\mathrm{sup}} - \dot{Q} \cdot \tilde{\theta}. \tag{7}$$

While this approach requires historical data of heat flow, supply and return temperature for model fitting, executing the model, for instance, as a surrogate in a physical simulation, reduces data requirements by needing only heat flow and supply temperature as inputs.

2.4.2. Application of the Model

For this study, reference data (see Section 2.3) for January and February were analyzed to target a period of high heat demand that covers the system's design operating range. Despite data cleaning and aggregation, intermittent data gaps persisted in several heating meter records. Consequently, the dataset was filtered to include 119 heating meters, each covering at least 85 % of the observed two-month timeframe.

Note that all subsequent steps were performed for each heating meter individually, yielding a distinct regression model per heating meter and, consequently, individualized return temperature predictions. The regression coefficients are reported in Table A1 in the Appendix A.

First, the coefficients of the model defined in Equation (6) must be determined, meaning a 'ground truth' for the response and predictor variables must be provided. For this purpose, the reference data was split chronologically using a continuous 80:20 split, reserving the first 80 % of the time series for model training (training dataset) and the remaining 20 % for testing and performance evaluation (test dataset). From the training dataset, 'true' θ-values were calculated using Equation (5). Additionally, the corresponding predictor variables $\frac{T_{\mathrm{sup}}}{\dot{Q}}$ and $\left(\frac{T_{\mathrm{sup}}}{\dot{Q}}\right)^2$ were computed. The so obtained variables were then used to fit the coefficients of the regression model, so that eventually a fully defined function for $\tilde{\theta}$ was available and $\tilde{T}_{\mathrm{ret}}$ was 'predicted' for the test dataset based on Equation (7). The overall procedure can be retraced in Figure 4.

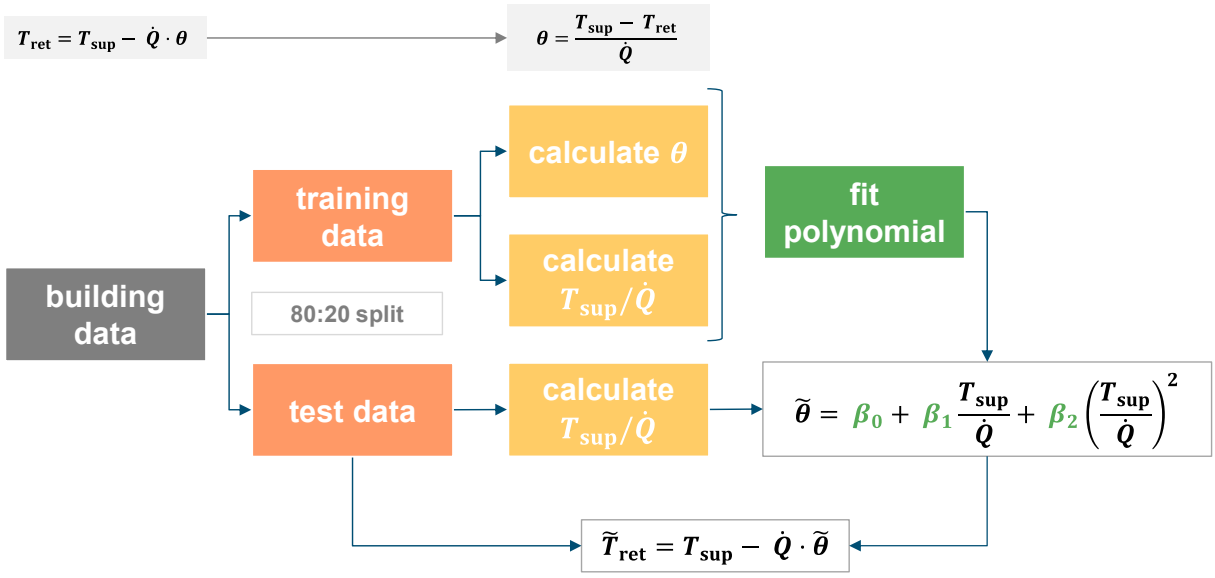


Figure 4. Schematic representation of return temperature prediction.

2.5. Analysis of Model Performance

The assessment of model performance was conducted based on the test dataset by pooling the results across all individual heating meters while simultaneously evaluating consistency across all heating meters. The analysis was performed separately for both $\tilde{\theta}$ and $\tilde{T}_{\mathrm{ret}}$. To capture both overall predictive quality and heating meter-level consistency, performance was evaluated by:

(1) Assessing systematic bias and structural dependencies via global residual analysis, residual scatter plots and the overall mean error (ME)

(2) Computing global error metrics:

   a. Quantifying overall goodness-of-fit and relative error scale using the coefficient of determination R^2

   b. Quantifying overall error magnitude using the mean absolute error (MAE), the root mean square error (RMSE) alongside the 95th percentile absolute error P_{95}.

(3) Assessing the dispersion of errors: Evaluating the dispersion of errors across heating meters and model stability across the individual heating meters m_i using the median of mean absolute error per-heating meter $median(\mathrm{MAE}_{m_i})$ and its interquartile range IQR.

All metrics were calculated based on:

- y_i: true value
- $\tilde{y}_i$: predicted value
- $\bar{y}$: mean of the true values
- n_{samples}: number of samples

Additionally, a comparison was conducted between the results obtained with the proposed method and the common assumption of a constant temperature difference between supply and return temperature. The details to this are elaborated in Section 3.3.

2.6. Systematic Bias and Residual Analysis

Systematic bias was evaluated through residual analysis, where residuals were computed as the difference of true and predicted values $e_i = y_i - \tilde{y}_i$ (corresponding to $\theta - \tilde{\theta}$ and $T_{\mathrm{ret}} - \tilde{T}_{\mathrm{ret}}$).

The global mean error (ME) was computed to verify overall model calibration:

$$\mathrm{ME} = \frac{1}{n_{\mathrm{samples}}} \sum (y_i - \tilde{y}_i). \tag{8}$$

Residuals tightly centered around zero ($\mathrm{ME} \approx 0$) indicate an unbiased model where prediction deviations are dominated by random noise rather than systematic under- or over-estimation. Additionally, residual plots against predicted values, true values, and input variables were examined. A random scatter around zero without visible curvature or clustering here likewise implies the absence of unmodeled non-linearities or structural dependencies. Conversely, visible patterns or systematic deviations may point to model misspecification.

2.7. Global Metrics

The global metrics were calculated on pooled data as follows:

$$\mathrm{R}^2 = 1 - \frac{\sum (y_i - \tilde{y}_i)^2}{\sum (y_i - \bar{y}_i)^2}, \tag{9}$$

$$\mathrm{MAE} = \frac{1}{n_{\mathrm{samples}}} \sum |y_i - \tilde{y}_i|, \tag{10}$$

$$\mathrm{RMSE} = \sqrt{\frac{1}{n_{\mathrm{samples}}} \sum (y_i - \tilde{y}_i)^2}. \tag{11}$$

To quantify tail-end deviations under heavy-tailed residual conditions the 95th percentile absolute error P_{95} was defined as the 0.95 empirical quantile of $|e_i|$.

2.8. Dispersion of Errors

To assess whether the global metrics were skewed by a subset of heating meters, per-heating meter statistics MAE_m and ME_m were computed for each heating meter m. Consistency across heating meters was evaluated via the median of all MAE_m alongside its interquartile range $\mathrm{IQR} = Q_{25} - Q_{75}$.

3. Results

This section presents the results obtained from applying the approach described in Section 2.4. Section 3.1 covers the results for the predictions of the scaling coefficient θ, followed by the corresponding analysis of the return temperature predictions in Section3.2. Additionally, the performance of the proposed method was compared with the assumption of a constant temperature difference in Section 3.3.

3.1. Evaluation of the Scaling Coefficient

Initially, the values of $\tilde{\theta}$ were calculated from all regression models (as described in Section 2.4.2) and are compared to the corresponding true values θ calculated directly from the reference data (see Section 2.3) according to Equation (5). Figure 5 shows the comparison of the predicted and true values for the test dataset, across all heating meters. The zoomed-in section covers the interquartile range of the data. The black line indicates a perfect agreement between predicted and true values, while the red dashed line represents a linear fit of the data cloud. The majority of the predicted values are located closely to the ideal line, with $97\ \%$ of the values falling within one standard deviation of the residual distribution and $98\ \%$ within two standard deviations. The overall coefficient of determination $R^2 = 0.98$ indicates that the regression models capture a large fraction of the variability in θ. Model accuracy is further supported by global error metrics, yielding $\mathrm{MAE} = 2 \times 10^{-4}\ \mathrm{K/W}$, $\mathrm{RMSE} = 9 \times 10^{-4}\ \mathrm{K/W}$ and $\mathrm{P}_{95} = 6 \times 10^{-4}\ \mathrm{K/W}$. The higher RMSE relative to MAE reflects the presence of occasional larger deviations. Across individual heating meters, performance remains consistent with a median of per-heating meter mean absolute errors $median(\mathrm{MAE}_m)$ of $0.6 \times 10^{-4}\ \mathrm{K/W}$ (IQR: $0.2 \times 10^{-4}\ \mathrm{K/W}$ to $1.1 \times 10^{-4}\ \mathrm{K/W}$).

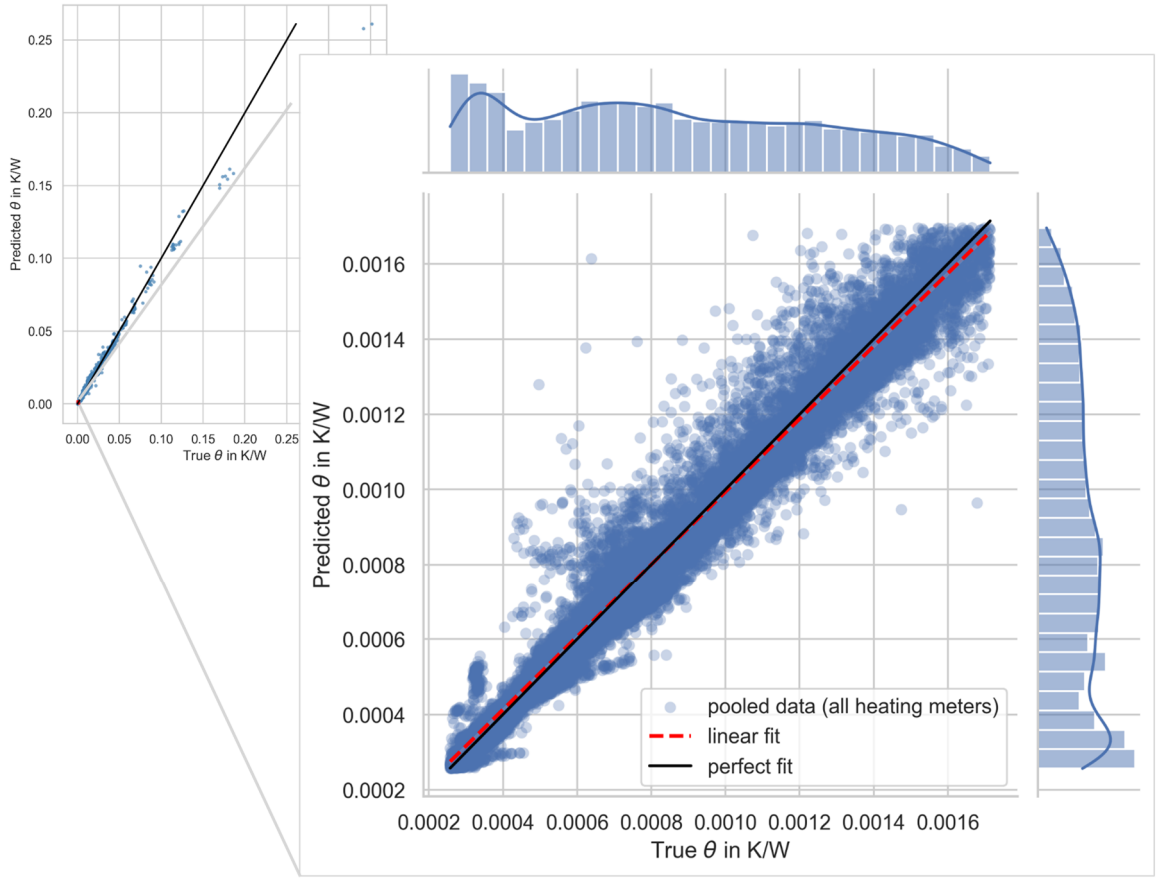


Figure 5. True vs. predicted values and density functions of θ (all heating meters)—zoomed into interquartile range.

The residual plots in Figure 6 reveal no significant systematic dependence of the residuals on the predicted θ-values (left), whereas a progressive underestimation appears for larger values of the predictor variable $\frac{T_{\mathrm{sup}}}{\dot{Q}}$ (right). However, the density profile reveals extreme data sparsity above $\frac{T_{\mathrm{sup}}}{\dot{Q}} = 0.02\ \mathrm{K/W}$, indicating that this apparent trend stems from a small number of high-leverage points. Within the main data range, the model exhibits no scale-dependent errors and adequately captures the dominant relationships between the predictor and response variable. Although prediction variance grows in sparse regions, the lack of data prevents drawing reliable

conclusions about true model performance at these extreme values. (Note that the plots were cropped to values within the interquartile range of $\tilde{\theta}$ with respect to the long tail of the density distribution to visualize systematic relationships within the relevant operating range.)

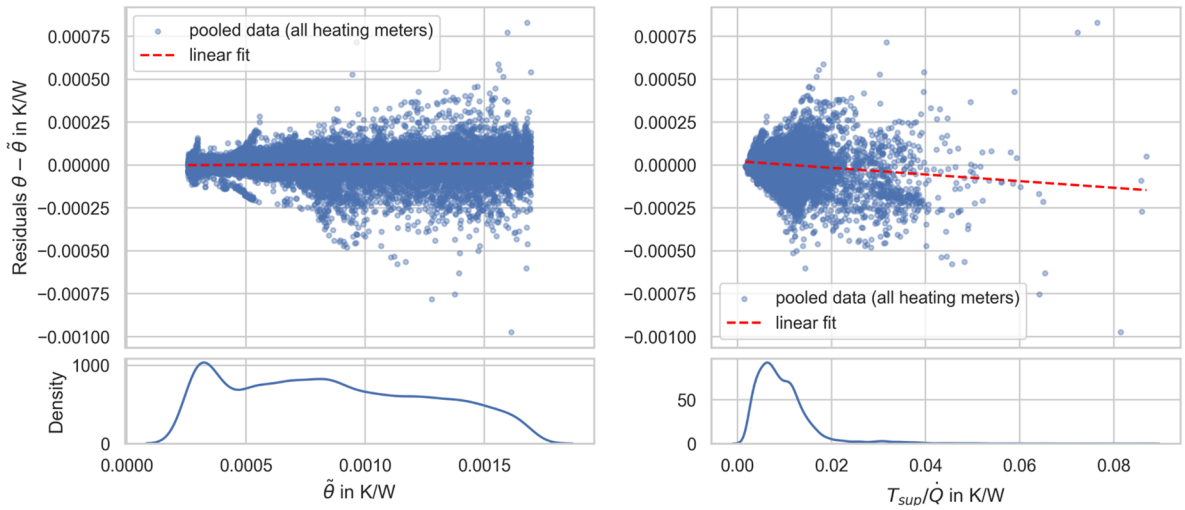


Figure 6. Residual plots for predicted values (**left**) and predictor values (**right**) with density representation—values that fall within interquartile range of the predicted values.

In summary, the residual analysis and error metrics indicate that the model provides an unbiased and robust prediction of θ across the dominant operating range, while deviations at the extremes can be attributed to limited data availability rather than structural model deficiencies.

3.2. Evaluation of the Predicted Return Temperature

The overall values of the return temperature predictions $\tilde{T}_{\mathrm{ret}}$ align well with our reference data T_{ret}, as can be seen in Figure 7, left. Most data points cluster around the line of perfect agreement (black), indicating high agreement between 'true' and 'predicted' values. However, at higher temperature ranges, the sparsity of data makes it difficult to assess whether prediction accuracy remains consistent.

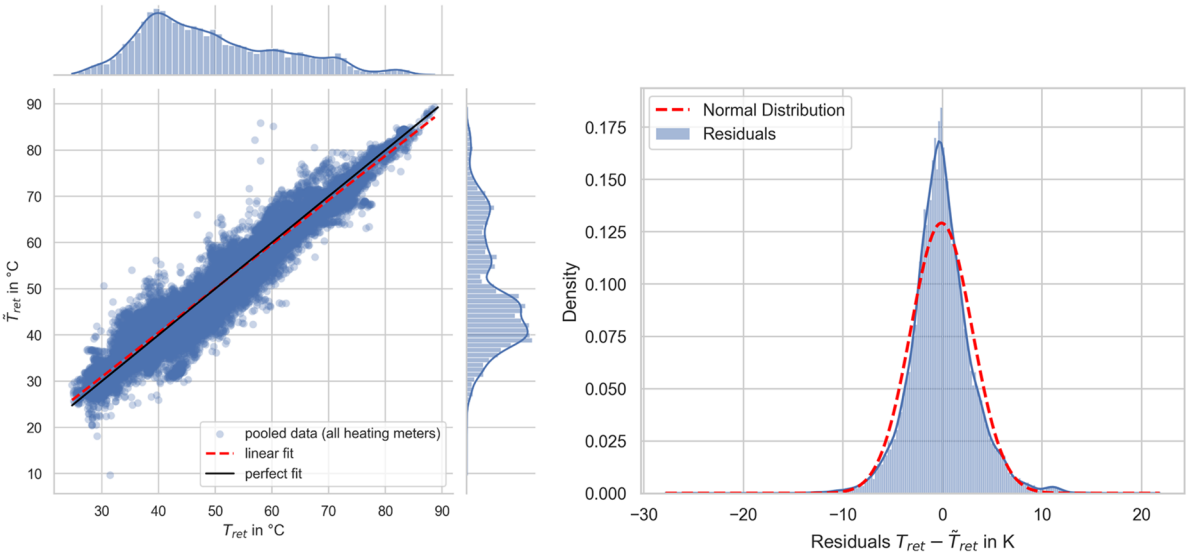


Figure 7. True vs. predicted values and density of return temperature values (**left**), Distribution of residuals (**right**).

As shown in Figure 7 (left), the predicted return temperatures exhibit strong agreement with the true values within the pooled dataset ($R^2 = 0.94$), demonstrating that the calculation preserves most of the predictive quality of the θ-approximation. The distribution of return temperature residuals (Figure 7, right) is tightly centered near zero with an overall mean error $\mathrm{ME} = -0.1$ K, indicating minimal systematic bias. Approximately 74 % of predicted values lie within one standard deviation (±3.1 K) and 96 % within two standard deviations (±6.2 K).

However, the residual distribution exhibits pronounced tails due to occasional large errors. The difference between the overall $\mathrm{MAE} = 2.3\ \mathrm{K}$ and $\mathrm{RMSE} = 3.1\ \mathrm{K}$ reflects the influence of these larger deviations, with a 95th-percentile absolute error P_{95} of 6.3 K. Individual performance across all heating meters remains consistent with a median of per-heating meter mean absolute errors $edian(\mathrm{MAE}_{m_i}) = 2.1\ \mathrm{K}$ (IQR: 1.6 K to 3.0 K).

The residual plots for the return temperatures are created as before, restricted to data points within the interquartile ranges, to account for the main data range. Figure 8 shows the return temperature residuals plotted against $\tilde{T}_{\mathrm{ret}}$ (left) and $\tilde{\theta}$ (right). In both diagrams, the fitted linear trendlines (red dashed) lie nearly flat around zero, and neither scatter plot exhibits severe scale-dependent drift or strong non-linear distortion, indicating that the transformation from $\tilde{\theta}$ to $\tilde{T}_{\mathrm{ret}}$ preserves unbiased predictions on average.

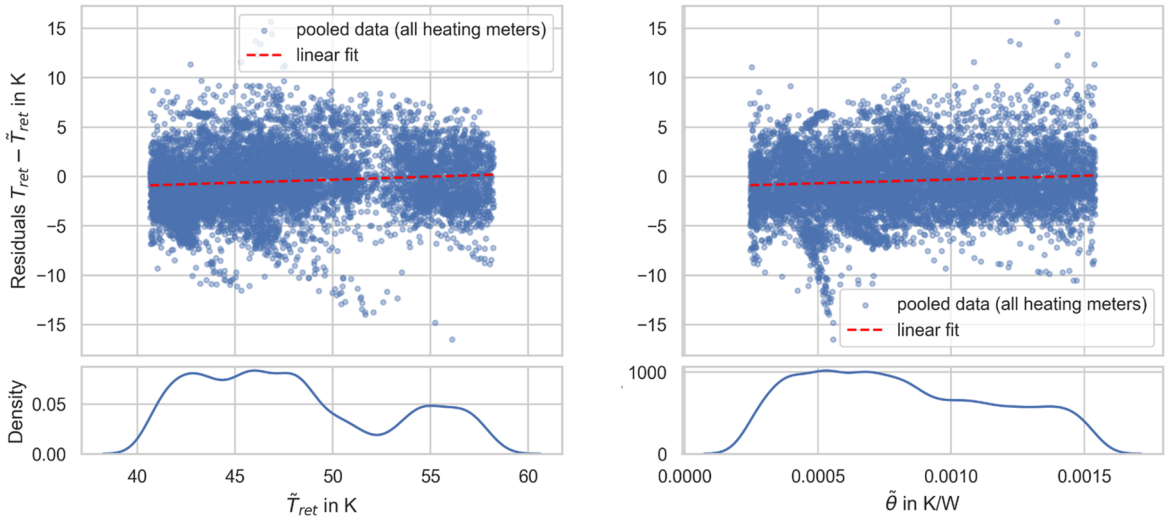


Figure 8. Residual plots for predicted return temperature values (**left**) and predicted θ-values (**right**)—cropped to values that fall into interquartile range.

Overall, the downstream calculation of return temperature shows no practically significant systematic bias and reproduces the central distributional characteristics of the test data well. The remaining residuals can largely be attributed to noise and data-related effects rather than structural deficiencies of the modeling approach.

3.3. Comparison with Constant Temperature Difference

To compare the proposed regression model against the common assumption of a constant substation temperature drop, both approaches were evaluated using the train–test split described in Section 2.4. Subtracting the mean temperature difference $\overline{\Delta T}$ of the training set from the test set supply temperature yielded the baseline return predictions. This baseline achieved an expectable high aggregate score over the pooled test data ($\mathrm{R}^2_{\overline{\Delta T}} = 0.89, \mathrm{MAE}_{\overline{\Delta T}} = 3.1\ °\mathrm{C}, \mathrm{RMSE}_{\overline{\Delta T}} = 4.2\ °\mathrm{C}$), which supports its widespread use in practice. However, because a constant temperature difference carries no dynamic system knowledge, its accuracy is highly sensitive to the selected averaging window; which might fail to generalize across changing operation regimes. Comparing individual heating meter-level error ranges achieved with a constant temperature difference ($MAE_{\overline{\Delta T}} \in [0.9,11.6]$) and the proposed regression model $\left(MAE_{\mathrm{reg}} \in [0.2,8.0]\right)$ demonstrates that incorporating substation-specific parameters into the regression model improves local accuracy. Accounting for these distinct substation properties is crucial for modulating operation scenarios and grid-level performance analyses.

4. Conclusions

In this work, we present a modelling approach with minimal dataset requirements by assuming that the return temperature can be expressed as the difference between the supply temperature and the transferred heat flow adjusted by a scaling coefficient. A polynomial regression model was used to fit this scaling coefficient to the aggregated heating meter data from a training dataset relying solely on primary side heat flow and supply temperature. After fitting individual models for each heating meter, scaling coefficient values were predicted for a test dataset, allowing to subsequently compute corresponding return temperature values. Model performance was evaluated with respect to systematic bias, correlations with input variables, distributional agreement between predicted and measured values as well as coefficients of determination.

The proposed approach yields practically unbiased estimates and high congruence with the 'true' data. This indicates that the dominant patterns present in the data are effectively captured by the model and that remaining deviations are largely attributable to noise in the measurement data. Nevertheless, the results also show that data density across the evaluated value range plays an important role in the regression fitting process, as prediction errors tend to increase in regions where data is sparse. In addition, although small in absolute magnitude, the error from the estimation of the scaling coefficient propagates to the subsequent return temperature calculation, underscoring the importance of input data quality. As the model formulation is grounded in basic thermodynamic relationships, fitting the regression models to data that are inconsistent with the underlying physical equations, due to operational faults, sensor errors, or inconsistent measurements, may impair prediction quality.

Furthermore, the use of a combined predictor that includes heat flow in the denominator introduces sensitivity to low heat flow values. At the same time, such values may carry limited information about system behavior, as they can arise from measurement noise during non-heating periods or from transient operating conditions such as start-up or shutdown phases. Consequently, excluding low heat flow values during model fitting or applying systematic data selection strategies that focus on operationally relevant regimes may improve model robustness and prediction accuracy. For handling missing data, smoothing techniques such as moving averages may be considered to reduce short-term fluctuations associated with system inertia, while avoiding excessive data manipulation that could obscure the underlying measurement characteristics.

Comparing the regression model to the conventional assumption of a constant temperature difference across a substation reveals similar performance on pooled data. However, the regression approach achieves higher overall accuracy and lower error metrics. While a constant temperature drop serves as a reasonable baseline during stable operating periods, it fails to capture dynamic system behavior across changing operational regimes. Individual heating meter evaluation shows that the regression model reduces the heating meter error ranges. This demonstrates that accounting for substation-specific physical properties is essential for accurate local performance analyses and modulation scenarios.

The findings of this study demonstrate the conceptual potential to simplify substation models within overall district heating network simulations using comparatively simple regression-based surrogate models. In contrast to many existing approaches, the proposed method relies exclusively on data that are typically available from primary side measurements, thereby improving applicability and transferability to real-world district heating systems. The results shall encourage scientists to critically assess the usefulness of sophisticated modeling approaches in favor of explainability and system understanding.

Future work may integrate a combination of established heat demand forecasting methods based on weather data with the proposed return temperature model. Such a combination could enable to ultimately create substation models that solely rely on input weather information, which corresponds to real-world system dependencies.

Author Contributions

J.E.: conceptualization, data curation, formal analysis, investigation, methodology, project administration, software, validation, visualization, writing—original draft, writing—review & editing; L.E.-K.: conceptualization, methodology, supervision, validation, writing—original draft, writing—review & editing; A.M.: methodology, supervision, writing—review & editing; F.D.: methodology, supervision, writing—review & editing; P.S.: conceptualization, funding acquisition, resources, supervision, writing—review & editing. All authors have read and agreed to the published version of the manuscript.

Funding

This research received no external funding.

Institutional Review Board Statement

Not applicable.

Informed Consent Statement

Not applicable.

Data Availability Statement

The data used in this work are available on reasonable request.

Conflicts of Interest

The authors declare no conflict of interest.

Use of AI and AI-Assisted Technologies

During the preparation of this work, the authors used ChatGPT (OpenAI), Gemini (Google), and DeepL Translator (DeepL SE) in order to improve language and readability. After using these tools, the authors reviewed and edited the content as needed and take full responsibility for the content of the publication.

Nomenclature

Variables	**Definition**	**Dimension**
β_0	Regression coefficient	K/W
β_1	Regression coefficient	-
β_2	Regression coefficient	W/K
$\frac{c_w}{\Delta T}$	Specific heat capacity of water	J/kgK
	Mean temperature difference	K
e	Residual	-
i	Index variable	-
$\theta, \tilde{\theta}$	True and predicted scaling coefficient	K/W
$\dot{m}$	Mass flow	kg/s
m_i	Heating meter i	-
n_{samples}	Number of samples	-
$\dot{Q}$	Heat flow	W
R^2	Coefficient of determination	-
S	Seasonal component	-
T	Trend component	-
t	time	s
$T_{\text{ret}}, \tilde{T}_{\text{ret}}$	True and predicted primary return temperature	K or °C
T_{sup}	Primary supply temperature	K
Y, y	Dataset value	-
Abbreviations		
ANN	Artificial neural network	
MAE	Mean absolute error	
ME	Mean error	
RMSE	Root mean squared error	

Appendix A

Table A1. Regression coefficients for $\tilde{\theta}$.

Heating Meter	$\boldsymbol{\beta_0}$	$\boldsymbol{\beta_1}$	$\boldsymbol{\beta_2}$
1	0.0001	0.061	−1.4849
2	−0.0001	0.115	0.6876
3	−0.0001	0.1327	−1.3993
4	−0.0002	0.1317	0.593
5	0	0.109	1.5284
6	0	0.095	0.5337
7	0.0001	0.1011	−0.0129
8	0	0.0757	2.1796
9	0.0001	0.0836	−1.0431
10	−0.0003	0.1606	−0.0624
11	−0.0001	0.12	0.8653
12	0	0.117	0.2094
13	0.0001	0.0899	0.0201
14	0.0003	0	0
15	−0.0003	0.1484	−2.3375
16	0.0001	−0.0179	1.7688
17	0.0001	0.0782	0.0024
18	0.0001	−0.002	0.0857
19	−0.0006	0.2443	−6.9746
20	−0.0002	0.1286	−0.0024
21	−0.0002	0.1678	−3.5203
22	−0.0085	0.33	−0.8748
23	−0.001	0.1394	−0.3844

Table A1. *Cont.*

Heating Meter	β_0	β_1	β_2
24	−0.0004	0.0987	−0.0034
25	0	0.1289	−0.6026
26	−0.0001	0.1198	0.4988
27	−0.0004	0.1138	−0.2482
28	−0.0008	0.1237	0.0067
29	0.0002	0.057	5.6342
30	0.0003	0.0164	0.0214
31	0.0001	0.0888	1.1863
32	−0.0002	0.1217	−0.5899
33	0	0.1132	−2.517
34	0	0.0684	0.6646
35	−0.0001	0.1452	−2.4158
36	−0.0003	0.1061	−0.0088
37	−0.0003	0.1358	−5.2188
38	−0.0003	0.1264	−1.3514
39	0.0001	−0.0039	3.4357
40	0.0001	0.0997	−0.242
41	−0.0001	0.1609	−11.8896
42	0	0.1307	−1.5954
43	0.0002	0.0076	1.0837
44	−0.0003	0.135	−0.7354
45	0	0.0481	−6.172
46	0	0.1371	−1.5633
47	−0.0001	0.1142	0.2674
48	0	0.036	79.9011
49	−0.0001	0.1277	−1.6414
50	−0.0002	0.1195	−0.0509
51	0	0.1238	−0.5405
52	−0.0001	0.2018	−20.4082
53	0.0005	0.033	0.1268
54	0.0001	−0.0087	3.245
55	−0.0008	0.1576	−0.9688
56	−0.0001	0.0859	−1.415
57	0.0002	0.0776	1.6174
58	−0.0002	0.2107	−35.6196
59	0.0001	−0.0716	73.3208
60	0	0.1141	−4.9008
61	0.0002	0.0173	−0.908
62	−0.0001	0.126	−5.9844
63	0.0001	0.0432	17.2862
64	0.0002	0.0514	−0.6753
65	0	0.0095	7.6337
66	−0.0001	0.1901	−24.1236
67	−0.0001	0.1351	−1.9597
68	−0.0002	0.2037	−3.5866
69	0	0.0846	−12.6347
70	0.0001	0.1399	−0.5045
71	0.0001	0.0445	−2.5005
72	−0.0015	0.2533	−2.1363
73	−0.0017	0.242	−1.431
74	0	0.0819	33.1991
75	0.0002	0.0457	0.3369
76	0	0.0647	−23.8004
77	0	0.1495	−20.144
78	0.0001	0.0692	1.0221
79	0	0.0869	0.8112
80	0.0002	0.1183	2.204
81	−0.0001	0.1673	−0.9387
82	−0.0001	0.1502	−2.778
83	−0.0008	0.194	−0.5334

Table A1. *Cont.*

Heating Meter	β_0	β_1	β_2
84	0.0005	0.093	0.0017
85	−0.0007	0.1818	−0.1304
86	0	0.0832	−0.6761
87	0.0018	0.0472	0.005
88	0	0.1595	0.2648
89	−0.0001	0.3492	−102.6027
90	0	0.077	5.5998
91	−0.0001	0.067	−2.5929
92	−0.0001	0.1456	−2.0818
93	−0.0002	0.2141	−10.6189
94	0	0.1214	0.3633
95	0	0.1411	4.4172
96	0	0.2143	−65.0057
97	0	0.0522	5.7322
98	0	0.1435	0.1087
99	−0.0009	0.235	−2.8775
100	−0.0001	0.1077	1.5393
101	0.0002	0.0979	0.4038
102	0	0.1489	0.4274
103	−0.0009	0.2015	−1.2374
104	0.0005	0.034	−0.0796
105	0.0001	0.0669	−6.3426
106	−0.0001	0.1614	−2.5712
107	0	0.122	8.0108
108	0.0001	0.0535	−0.3535
109	0	0.1093	−1.2093
110	0.0006	0.0108	0.0201
111	0.0007	0.0924	−0.4453
112	−0.0002	0.1911	−1.989
113	−0.0003	0.1226	0.3581
114	−0.0001	0.1309	−2.1198
115	−0.0003	0.1317	−2.0393
116	−0.0009	0.135	−0.2025
117	0.0002	−0.0206	9.2254
118	−0.0001	0.2054	−16.309
119	0	0.0563	−0.1008

References

1. Werner, S. International review of district heating and cooling. *Energy* **2017**, *137*, 617–631. https://doi.org/10.1016/j.energy.2017.04.045.
2. Westermann, P.; Evins, R. Surrogate modelling for sustainable building design—A review. *Energy Build.* **2019**, *198*, 170–186. https://doi.org/10.1016/j.enbuild.2019.05.057.
3. Østergård, T.; Jensen, R.L.; Maagaard, S.E. A comparison of six metamodeling techniques applied to building performance simulations. *Appl. Energy* **2018**, *211*, 89–103. https://doi.org/10.1016/j.apenergy.2017.10.102.
4. Zouloumis, L.; Stergianakos, G.; Ploskas, N.; et al. Dynamic Simulation-Based Surrogate Model for the Dimensioning of Building Energy Systems. *Energies* **2021**, *14*, 7141. https://doi.org/10.3390/en14217141.
5. Boussaid, T.; Rousset, F.; Scuturici, V.M.; et al. Enabling fast prediction of district heating networks transients via a physics-guided graph neural network. *Appl. Energy* **2024**, *370*, 123634. https://doi.org/10.1016/j.apenergy.2024.123634.
6. Zhao, H.X.; Magoulès, F. A review on the prediction of building energy consumption. *Renew. Sustain. Energy Rev.* **2012**, *16*, 3586–3592. https://doi.org/10.1016/j.rser.2012.02.049.
7. Fang, T.; Lahdelma, R. Evaluation of a multiple linear regression model and SARIMA model in forecasting heat demand for district heating system. *Appl. Energy* **2016**, *179*, 544–552. https://doi.org/10.1016/j.apenergy.2016.06.133.
8. Oltmanns, J.J. Analysis and Improvement of an Existing University District Energy System. Ph.D. Thesis, Technical University of Darmstadt, Darmstadt, Germany, 2021. https://doi.org/10.26083/tuprints-00017367.
9. Popescu, D.; Ungureanu, F.; Hernández-Guerrero, A. Simulation models for the analysis of space heat consumption of buildings. *Energy* **2009**, *34*, 1447–1453. https://doi.org/10.1016/j.energy.2009.05.035.

10. Werner, S. District Heating and Cooling. In *Reference Module in Earth Systems and Environmental Sciences*; Elsevier: Amsterdam, The Netherlands, 2013. https://doi.org/10.1016/b978-0-12-409548-9.01094-0.
11. Vandermeulen, A.; Van Oevelen, T.; van der Heijde, B.; et al. A simulation-based evaluation of substation models for network flexibility characterisation in district heating networks. *Energy* **2020**, *201*, 117650. https://doi.org/10.1016/j.energy.2020.117650.
12. Schweiger, G.; Larsson, P.-O.; Magnusson, F.; et al. District heating and cooling systems—Framework for Modelica-based simulation and dynamic optimization. *Energy* **2017**, *137*, 566–578. https://doi.org/10.1016/j.energy.2017.05.115.
13. Ikonen, E.; Selek, I.; Kovacs, J.; et al. Short term optimization of district heating network supply temperatures. In Proceedings of the IEEE International Energy Conference (ENERGYCON), Cavtat, Croatia, 13–16 May 2014; pp. 996–1003. https://doi.org/10.1109/energycon.2014.6850547.
14. Laakkonen, L.; Korpela, T.; Kaivosoja, J.; et al. Predictive Supply Temperature Optimization of District Heating Networks Using Delay Distributions. *Energy Procedia* **2017**, *116*, 297–309. https://doi.org/10.1016/j.egypro.2017.05.076.
15. Leśko, M.; Bujalski, W.; Futyma, K. Operational optimization in district heating systems with the use of thermal energy storage. *Energy* **2018**, *165*, 902–915. https://doi.org/10.1016/j.energy.2018.09.141